Atmos. Chem. Phys. Discuss., 14, 20417–20460, 2014
www.atmos-chem-phys-discuss.net/14/20417/2014/
doi:10.5194/acpd-14-20417-2014

Atmospheric Chemistry and Physics
Discussions
Open Access

Nitrous oxide emissions from a commercial cornfield (*Zea mays*) measured using the eddy-covariance technique

H. Huang[1], J. Wang[1], D. Hui[2], D. R. Miller[3], S. Bhattarai[2], S. Dennis[2], D. Smart[4], T. Sammis[5], and K. C. Reddy[2]

[1]Climate Science Section, Illinois State Water Survey, Prairie Research Institute, University of Illinois at Urbana-Champaign, Champaign, IL 61820, USA
[2]College of Agriculture, Human and Natural Sciences, Tennessee State University, Nashville, TN 37209, USA
[3]Department of Natural Resources and Environment, University of Connecticut, Storrs, CT 06269, USA
[4]Department of Viticulture and Enology, University of California, Davis, CA 95616, USA
[5]Department of Plant and Environmental Science, New Mexico State University, Las Cruces, NM 88003, USA

Received: 17 May 2014 – Accepted: 22 July 2014 – Published: 8 August 2014

Correspondence to: J. Wang (wangjim@illinois.edu)

Published by Copernicus Publications on behalf of the European Geosciences Union.

Abstract

Increases in observed atmospheric concentrations of the long-lived greenhouse gas, nitrous oxide (N_2O), have been well documented. However, information on event-related instantaneous emissions during fertilizer applications is lacking. With the development of fast-response N_2O analyzers, the eddy covariance (EC) technique can be used to gather instantaneous measurements of N_2O concentrations to quantify the exchange of nitrogen between the soil and atmosphere. The objectives of this study were to evaluate the performance of a new EC system, to measure the N_2O flux with the system, and finally to examine relationships of the N_2O flux with soil temperature, soil moisture, precipitation, and fertilization events.

We assembled an EC system that included a sonic anemometer and a fast-response N_2O analyzer (quantum cascade laser spectrometer) in a cornfield in Nolensville, Tennessee during the 2012 corn growing season (4 April–8 August). Fertilizer amounts totaling 217 kg N ha^{-1} were applied to the experimental site. The precision of the instrument was 0.066 ppbv for 10 Hz measurements. The seasonal mean detection limit of the N_2O flux measurements was 2.10 ng N m^{-2} s^{-1}. This EC system can be used to provide reliable N_2O flux measurements. The cumulative emitted N_2O for the entire growing season was 6.87 kg N_2O-N ha^{-1}. The 30 min average N_2O emissions ranged from 0 to 11 100 µg N_2O-N m^{-2} h^{-1} (mean = 257.5, standard deviation = 817.7). Average daytime emissions were much higher than night emissions (278.8 ± 865.8 vs. 100.0 ± 210.0 µg N_2O-N m^{-2} h^{-1}). Seasonal fluxes were highly dependent on soil moisture rather than soil temperature, although the diurnal flux was positively related to soil temperature. This study was one of the few experiments that continuously measured instantaneous, high-frequency N_2O emissions in crop fields over a growing season of more than 100 days.

ACPD

14, 20417–20460, 2014

1 Introduction

As the largest corn producer in the world, the United States produces about one-third of the world's corn crop (about 34 million ha in 2011) (http://www.epa.gov/agriculture/ag101/cropmajor.html). Corn is a nitrogen (N) intensive crop. Every year, large amounts of N are applied to cornfields, but the nitrogen use efficiency is low (30–59 %) (Halvorson et al., 2005). Consequently, a large proportion of applied N can be leached to groundwater as NO_3^- and/or emitted to the atmosphere as nitrous oxide (N_2O), nitric dioxide (NO), or nitrogen dioxide (NO_2).

N_2O is one of the longest lived greenhouse gases (GHGs), has an estimated radiative forcing of $0.15\,W\,m^{-2}$, compared to carbon dioxide (CO_2) at $2.43\,W\,m^{-2}$ and methane (CH_4) at $0.48\,W\,m^{-2}$ (Forster et al., 2007). In addition to its contribution to global warming, N_2O also plays an important role in stratospheric ozone depletion through O (1-D) oxidation (Ravishankara et al., 2009). The volume concentration of N_2O in the atmosphere has increased from 273 parts per billion dry air mole fraction (ppbv) in 1750 to 319 ppbv in 2005 (Forster et al., 2007). The major source of anthropogenic N_2O in the atmosphere is believed to be N fertilization accounting for up to 80 % of anthropogenic N_2O emissions (Kroeze et al., 1999; Mosier et al., 1998). N_2O emitted from soil is produced by bacterial processes, mainly through nitrification and denitrification (Davidson and Swank, 1986). These processes may be affected by several factors, including the percentage of water-filled pore spaces in soil (WFPS) (Dobbie and Smith, 2003; Davidson, 1991), mineral N concentrations in the soil (Ma et al., 2010; Bouwman et al., 2002; Bouwman, 1996), crop type, soil type, soil moisture, air/soil temperature, and oxygen supply. Therefore, N_2O emissions are typically highly variable both in time and space, and are difficult to quantify.

Significant efforts have been invested in developing reliable tools for measuring instantaneous N_2O emissions from soil to the atmosphere. The two major measurement methods currently available for N_2O flux are the chamber method and the eddy covariance (EC) method (Molodovskaya et al., 2011; Denmead, 2008). The chambers,

ACPD
14, 20417–20460, 2014

either closed (static) or open (dynamic flow), are the traditional tools that have been used in different land management systems (farmland, forest, and grassland) (Tao et al., 2013; Liu et al., 2012; Arnolda et al., 2005; Klemedtsson et al., 1996). The chamber method is simple in concept and operation, as well as low in cost. However, several limitations may affect the data quality, such as small area coverage, called the footprint, ($\leq 1\,m^2$), disturbance of the soil environment, and low sampling frequency (Molodovskaya et al., 2011; Denmead, 2008). The EC method calculates the spatial averaged flux from a larger field scale footprint ($10\,m^2$–$1\,km^2$), unlike the chamber method, the EC method does not disturb the soil and crop ecosystem and provides a continuous and real-time flux measurement (Denmead, 2008).

The EC method is based on the Reynolds decomposition theory that a turbulent variable (x) can be represented by a time-averaged component ($\overline{x}$) and a fluctuation component (x') (Famulari et al., 2010; Kaimal and Finnigan, 1994; Stull, 1988):

$$x = \overline{x} + x'. \tag{1}$$

In the EC method, the vertical flux of a gas is expressed as the covariance between the vertical wind velocity and gas concentration fluctuations:

$$J = \overline{\varpi' c'} \tag{2}$$

where J is the gas vertical flux, ϖ' and c', are the deviations of vertical wind velocity (ϖ) and gas concentration (c), respectively and the overbar represents a time average. The EC method requires rapid, simultaneous (or near-simultaneous) measurements of gas concentration and wind velocity at the same point in space. Previous N_2O analyzer instruments lacked the necessary precision and their response times were too slow for use in EC measurements. With the developments of fast-response N_2O analyzers in recent years, the EC method has become more common (Jones et al., 2011; Mammarella et al., 2010; Eugster et al., 2007; Pihlatie et al., 2005; Marco et al., 2004; Edwards et al., 2003). In this project, an EC system for N_2O measurement was assembled in a commercial cornfield in Nolensville (TN) with a newly available fast-response

ACPD
14, 20417–20460, 2014

N_2O analyzer. N_2O analyzer, quantum cascade laser (QCL) spectrometer (model CW-QCTILDAS-76-CS, Aerodyne Research Inc., Billerica MA).

The objectives of this study were to evaluate the performance of the new N_2O spectrometer in the EC system, to measure the N_2O flux with the system, and finally to examine relationships between the N_2O flux and soil temperature, soil moisture, precipitation, and fertilization events.

2 Materials and methods

2.1 Site description

The experimental site was located in a commercial cornfield in Nolensville, Tennessee, 35 km south of Nashville (Fig. 1). The field was 300 m (east–west) by 500 m (south–north) with a 2 % slope facing west. The soil type was Talbott silty clay loam (Fine, mixed, semi-active, thermic Typic Hapludalfs; 32.5 % sand, 53.8 % silt, 13.8 % clay) (http://websoilsurvey.nrcs.usda.gov/app/WebSoilSurvey.aspx). Soybeans were planted in the previous year's rotation. Corn seeds (Roundup Ready BT Hybrid Corn, P1412 HR, Pioneer Hi-Bred International Inc., Johnston, IA) were sown on 9 April 2012. Measurements were continuous from 4 April to 8 August 2012, covering the entire corn-growing season.

The agricultural practice was no-till. A weather station (Vantage PRO2 Plus, Davis Instruments, Vernon Hills, IL) was used to record 30 min precipitation, temperature, pressure, wind speed and direction, relative humidity (RH), and solar radiation. The prevailing wind direction was from the southwest during the growing season.

2.2 The EC instruments

A sonic anemometer (CSAT3-A, Campbell Sci, Logan, UT) located in the middle of the field, measured three-dimensional wind velocities and virtual air temperatures at a sampling rate of 10 Hz. It was positioned 1.3 m above the canopy, and was raised

ACPD
14, 20417–20460, 2014

as the corn plants grew taller. N_2O concentrations were measured by a quantum cascade laser (QCL) spectrometer (model CW-QC-TILDAS-76-CS, Aerodyne Research Inc., Billerica, MA). The N_2O analyzer was housed in a trailer where a stable working temperature (293–303 K) was maintained. The pressure of the spectrometer sample cell was 4 kPa (30 Torr). The laser was operated at a wavelength of 2193 cm^{-1}.

The N_2O analyzer was located 50 m from the sonic anemometer. Following the specifications of Eugster et al. (2007), a sampling Teflon tube (6 mm inner diameter, 50 m length) was used to sample the air at the EC sonic anemometer location in the middle of the field and was connected to the N_2O analyzer. The tube intake was 20 cm from the sonic anemometer. Sample air was drawn into the tube intake at a rate of 14 STD L min^{-1}. The analyzer provided 10 Hz measurements of N_2O and water vapor (H_2O) concentrations. The analyzer automatically corrected the H_2O effects on N_2O measurements (WPL and cross-sensitivity of H_2O on N_2O) in real time (Nelson, 2002). A Campbell Scientific CR3000 data logger was used to record all the data collected at 10 Hz. The EC measurement footprint ranged from 25 to 90 m upwind, and was calculated using the software EddyPro (version 3.0, LI-COR Biosciences, Lincoln, NE). Soil moisture and soil temperatures were measured with a water content reflectometer (CS616) and an averaging soil thermocouple probe (TCAV, Campbell Sci, Logan, UT), which were buried vertically at a depth of 0–10 cm underground. The mineral NO_3^- and NH^+ concentrations in the top 10 cm of soil were measured using a Lachat Flow Injection Auto-analyzer (Loveland, CO).

2.3 N_2O flux calculation and data corrections

The EddyPro version 3.0 was used to process and correct the N_2O flux. EC fluxes were calculated as the covariance of the fluctuations of vertical wind velocity and N_2O concentration over an averaging period:

$$J_{N_2O} = \overline{\omega' c'_{N_2O}} \cdot \frac{\rho_a}{M_a} \cdot 3600 \cdot 28 \times 10^{-3}, \tag{3}$$

ACPD
14, 20417–20460, 2014

Nitrous oxide emissions from a commercial cornfield

H. Huang et al.

where J_{N_2O} is the N_2O flux (µg N_2O–N m^{-2} h^{-1}), c_{N_2O} is the N_2O concentration in air (ppbv), the component prime (′) indicates a deviation from the mean, and the overbar denotes a time average, ρ_a is the density of air (kg m^{-3}) and M_a is the molar mass of air (0.028965 kg mol^{-1}), 3600 represents 3600 s h^{-1}, and 28 is the molar mass of two N atoms in N_2O (g $mole^{-1}$).

The averaging period to determine eddy fluxes must be sufficient to adequately sample all the motions that contribute to the fluxes, but an overly long averaging period might affect measurements with irrelevant signals. According to Moncrieff et al. (2004), an averaging period of 30 to 60 min is appropriate for gas flux calculations. In this study, a commonly used averaging period of 30 min was chosen (Mammarella et al., 2010; Eugster et al., 2007; Aubinet et al., 2000).

EC measurements need several corrections before and after performing a flux calculation. Data spikes can be caused by random electronic spikes in the measuring or recording systems. The de-spike procedure was applied to the raw data (10 Hz) before the calculation of flux. The spike detection and removal method used in this study was similar to that of Vickers and Mahrt (1997). A spike was identified as up to 3 consecutive outliers with respect to a plausible range within a certain time range, and the spike was replaced with the linear interpolation between adjacent data points. The rationale is that if more consecutive values are found to exceed the plausibility threshold, they might be a sign of an unusual yet physical trend (not an outlier) (Eddypro Version 3.0, 2012). The threshold was set to 3 to 8 times the standard deviation for a given averaging period (3 times for wind velocity and air temperature, and 8 times for N_2O concentrations; these parameters represent the default values in EddyPro).

The vertical axis of the sonic anemometer was not always aligned with the local normal to the surface. Therefore, there could be cross-contamination among components of the flux divergence. In order to avoid cross-contamination, an axis rotation was necessary. The EddyPro used a double rotation scheme, in which the u-component was aligned with a local streamline for each 30 min interval, and the v-component and ω-component were forced to be zero on average.

The physical separation of the sonic anemometer and the N_2O analyzer caused a time lag (τ) between the sonic data and N_2O data. Compensation for τ before the covariance calculation is required in the EC technique. In this study, the τ for each 30 min averaging period was obtained by searching for the maximum cross covariance between sonic variables and analyzer measurements.

All EC systems tend to underestimate the true atmospheric fluxes due to physical limitations of the instruments which cause flux losses at high (e.g., damping effects from long intake tube) and low frequencies. The commonly used methods of addressing spectral attenuation have been described in Ferrara et al. (2012) and Moncrieff et al. (2004). The EddyPro provides several options for spectral correction. In this study at the low frequency range, the analytic correction proposed by Moncrieff et al. (2004) was used, and at the high frequency range, the spectral loss was corrected following Ibrom et al. (2007) and Horst and Lenschow (2009).

The frequency loss ratio ($\frac{\Delta\emptyset}{\emptyset}$) was calculated as:

$$\frac{\Delta\emptyset}{\emptyset} = 1 - \frac{\int_0^{+\infty} \mathrm{CO}_M \mathrm{d}f}{\int_0^{+\infty} \mathrm{CO}_T \mathrm{d}f} \tag{4}$$

where the CO_T is the theoretical N_2O flux cospectra following Kaimal et al. (1972), CO_M is the N_2O flux cospectra from the measured data, and f is the spectral frequency.

The EddyPro outputs a frequency correction factor for N_2O (N_2O–cf) as the ratio of the frequency-corrected flux divided by the flux before the frequency correction. Therefore the frequency correction ratio by EddyPro ($\frac{\Delta\emptyset}{\emptyset}$(EP)) is:

$$\frac{\Delta\emptyset}{\emptyset}(\mathrm{EP}) = 1 - \frac{1}{\mathrm{N_2O{-}cf}} \tag{5}$$

2.4 Data for weak turbulence and precipitation conditions

It has been found that under weak wind conditions with no surface heating, turbulence may not develop. Friction velocity (u^*) was used to measure the turbulent state of the

ACPD
14, 20417–20460, 2014

atmosphere:

$$u^* = (\overline{\omega' u'^2} + \overline{\omega' v'^2})^{\frac{1}{4}}, \tag{6}$$

where u' and v' are the fluctuations in horizontal downwind and crosswind components.

The determination of an adequate u^* threshold for sufficient turbulent mixing was crucial. The common method to determine the u^* threshold is to examine the scatter plot of night time flux vs. u^*, and the threshold is located at the point in which the flux begins to level off as u^* increases (Gu et al., 2005). There are also many statistic-based algorithms used to determine u^* thresholds (Papale et al., 2006; Gu et al., 2005; Saleska et al., 2003). Mammarella (2011) summarizes the appropriate range of the u^* threshold as 0.1 for grassland to 0.3 for forest. In this study we used 0.2 as the threshold for the cornfield.

During precipitation conditions, the sonic anemometer sensor heads could be wet, causing errors in the instantaneous measurements. Therefore, in this study the N_2O flux data were excluded in low turbulence, $u^* < 0.2\,\mathrm{m\,s^{-1}}$, and during rainfall.

2.5 Measurement periods

As noted above, continuous measurements were carried out from 4 April to 8 August 2012. The corn was harvested one week after the study period ended. On 8 August, the moisture content of the kernels was less than 25 %; therefore the study period covered the entire growing season. Prior to planting and before the EC measurements were initiated, chicken litter (99 $\mathrm{kg\,N\,ha^{-1}}$) was applied to the field on 10 March. Two applications of fertilizers were subsequently supplied on 10 April (URAN-32-0-0 liquid nitrogen, 39 $\mathrm{kg\,N\,ha^{-1}}$) and 14 May (URAN-32-0-0 liquid nitrogen, 79 $\mathrm{kg\,N\,ha^{-1}}$). The experimental period was divided into four specific periods based on fertilization or precipitation events (Table 1). The first period started 24 days after the application of chicken litter and the first liquid fertilizer application was within this period. The second period was characterized by the second fertilizer application and high precipitation. The third period was without fertilization and significant precipitation, and the fourth period had high relative precipitation but no fertilization. The data were further divided into two groups according to the measurement time: daytime (7 a.m. to 7 p.m.) and night time (7 p.m. to 7 a.m.). Mean and standard deviation of the N_2O flux, soil moisture, and soil temperature were obtained. Regression and correlation analysis were conducted for day and night for different temporal periods. The regression equations were used for filling gaps at the missing data points. The N_2O flux was then integrated for the whole season to obtain the overall N_2O emission.

3 Results

3.1 The performance of the N_2O analyzer

The precision of the N_2O concentration measurements was characterized under field sampling conditions by the Allan variance technique (Fig. 2). In the log-log plot, the measurement variance decreased with the integration time (t) with a slope of -1 when $t \leq 10$ s, indicating that there were no correlations between noise sources (pink noise) at time scales of 0.1 to 10 s. The variance had a broad minimum between 10 and 100 s with a minimum corresponding to 0.006 ppbv of standard deviation. The standard deviation was 0.066 ppbv for 10 Hz (integration time 0.1 s), 0.020 ppbv for 1 Hz (integration time 1 s), and 0.006 ppbv for 0.1 Hz (integration time 10 s).

Figure 3 shows the frequency distribution of time lags during the experimental period. The peak value of the distribution appeared at $\tau = 6.3$ s, which represented the air flow time in the sampling tube between the field collection location and the QCL N_2O analyzer.

Figure 4 shows sample cospectra of sensible heat and N_2O and the theoretical N_2O cospectra obtained during a windy day (Fig. 4a) and a windy night (Fig. 4b). A rather good performance of the N_2O cospectrum in the low frequencies was demonstrated. The N_2O cospectrum fell off faster at higher frequencies than the theoretical cospectrum and the sensible heat cospectrum. The N_2O flux frequency loss ratios during the daytime and night time were low (1 % and 2 %). The frequency correction ratios by EddyPro for the daytime and night time were 18 and 19 %, respectively.

Table 2 shows the variation of the frequency loss ratio of N_2O flux under weak to strong wind conditions (u^* is linearly related to wind speed). In general, the mean of flux frequency loss ratios (including all ratios: ≥ 0 and < 0) increased with increased wind speed (u^*) when $u^* < 0.2\,\mathrm{m\,s^{-1}}$. When $u^* < 0.2\,\mathrm{m\,s^{-1}}$, the eddies may not have been well enough developed for the measurements to be accurate. Under the night time condition, the frequency loss ratio was larger than under the daytime condition when the u^* values were in the same category. The average EddyPro frequency correction ratio was 15–18 %.

3.2 Seasonal variations

A total of 5,197 30 min data units were collected. After applying the two filters ($u^* \geq 0.2$, precipitation free), 1390 data units remained. In general, the concentration and the flux of N_2O had higher values during and after the fertilizer application but gradually decreased with time, as shown in Figs. 5 and 6. However, rainfall (soil moisture) was a trigger for N_2O emissions, which is the reason the flux reached peak values on the day of the largest application of URAN-32-0-0 (14 May), and the lack of peak values of N_2O flux just after the first application with no rainfall. The growing season was characterized by a number of precipitation events which appeared to increase the N_2O concentration as well as the N_2O flux.

Note the two general seasonal concentration levels in Fig. 6. One was before a continuous corn canopy was established in early June, and the second, with a continuous canopy extended from mid-June to 8 August. These may have been caused by the high applications of the fertilizer and less N use by the establishing crop before June which resulted in higher soil N availability and more N_2O emissions during that period as shown in Fig. 5.

ACPD
14, 20417–20460, 2014

3.3 Diurnal variations

Diurnal variations of the N_2O flux were detected (Fig. 7). The peak flux commonly appeared during the daytime, whereas the flux was low at night except for the third sub-period when soil moisture was high during the night time. The average daytime and night time N_2O fluxes during the whole season were 278.8 ± 865.8 and $100.0 \pm 210.0\,\mu g\,N_2O{-}N\,m^{-2}\,h^{-1}$, respectively. This diurnal response was most likely a temperature response superimposed on the longer term variations due to slowly changing soil moisture content as noted below in Sect. 3.5.

3.4 Result statistics

The N_2O concentrations and fluxes were highly variable with time. The concentration was 322.9 ± 4.0 ppbv with a coefficient of variation (CV) of 1.24 %. The N_2O flux ranged from 0.0 to event-related emissions as high as $11\,100\,\mu g\,N_2O{-}N\,m^{-2}\,h^{-1}$ with a CV of 317.6 % and a mean of $257.5 \pm 817.7\,\mu g\,N_2O{-}N\,m^{-2}\,h^{-1}$. The concentrations and fluxes exhibited skewed distributions with higher means than medians. As shown in Table 3, nearly 90 % of the data were obtained during the daytime. Both concentrations and fluxes were higher during the daytime than during the night. For the whole experimental period, the total emission was $6.87\,kg\,N_2O{-}N\,ha^{-1}$ (Fig. 8).

3.5 Effects of soil moisture, temperature, and N availability on N_2O emissions

Figure 9 presents an overview of the measured concentration and flux for the whole experimental period, together with soil temperature and soil moisture. Generally, the variations of N_2O concentration and flux followed most closely the pattern of variation of soil moisture. As expected, concentrations and fluxes were usually elevated immediately after precipitation events. As shown in Table 1, there was no fertilization event or significant precipitation in the third period, and thus the N_2O flux was constantly low.

In previous studies it has been difficult to generalize and interpret the relationships of N_2O emissions with soil temperature or soil moisture quantitatively because in each specific study the determinants are different. In this study, for the entire experimental period, the N_2O flux was positively correlated to soil moisture with a Pearson correlation coefficient r of 0.42 ($p < 0.001$), while the correlation with soil temperature was poor ($r = -0.079$, $p = 0.003$). Table 4 shows the Pearson correlation coefficients for the periods defined in Table 1. The N_2O flux was significantly correlated with soil moisture except for S1N, which was probably limited by the small sample size. These correlations indicate that on this site the dominant driver of N_2O emissions was soil moisture in addition to substrate availability (N fertilization).

Although the soil temperature did not positively correlate to the seasonal N_2O emission, it was significantly and positively correlated to the diurnal (hourly) N_2O emission during the first and second sub-periods (correlation coefficient $r_{st} = 0.76$ and 0.56, $p < 0.001$) when soil moisture was not strongly predictive ($r_{sm} < 0.36$, $p > 0.05$) (Fig. 7). Therefore, the peak flux during these sub-periods appeared most often during the day when the soil temperature was relatively high compared to the night. However, during the times of significant effects of soil moisture ($r_{sm} > 0.45$, $p < 0.05$) (the third and fourth sub-periods), the temperature effects on the N_2O flux were not significant ($r_{st} < 0.2$, $p > 0.05$).

Several studies have found that N_2O flux increased exponentially with soil temperature (Dinsmore et al., 2009; Schindlbacher et al., 2004; Smith et al., 2003). At first we regressed the observed N_2O flux with soil temperature and soil moisture following the exponential functions given by Luo et al. (2013). However, for some periods the coefficients of determination (R^2) were low (< 0.4). Then we regressed the N_2O flux with soil temperature and soil moisture using exponential or polynomial functions (Table 5). The values of R^2 ranged from 0.45 to 0.70. For most of the periods, soil moisture explained a significant amount of the variation in N_2O emissions.

N availability was an important factor in N_2O emissions. The fertilizer amount of the second application was more than twice that of the first application; the large amount of fertilizer provided sufficient N^+. The volume concentration of NO_3^- in the top 10 cm of soil was 5.5 ppmv on 15 April, and was 8.5 ppmv on 16 May. The concentrations of NH^+ were 16 ppmv and 19.5 ppmv for these two days, respectively. The higher mineral N^+ concentration most likely contributed to the dramatic increase in N_2O concentration and flux after the second application.

4 Discussion

4.1 N_2O analyzer performance

Several studies have been performed for N_2O measurements using QCL spectrometers over grassland or forest (Neftel et al., 2010, 2007; Eugster et al., 2007; Kroon et al., 2007; Nelson et al., 2004, e.g.). Besides experimental locations, seasons, and/or crop types, the instruments utilized in these studies differed from each other in terms of absorption line and precision. For example, in the studies of Kroon et al. (2007) and Neftel et al. (2010), N_2O was measured at wavelengths of 1271.1 cm^{-1} and 1275.5 cm^{-1}, respectively, while in Neftel et al. (2007) and Eugster et al. (2007) N_2O was measured at 2241.0 cm^{-1} and 2243.1 cm^{-1}, respectively. The precision of the instruments in these four studies, at a sampling rate of 1 Hz, was 0.5, 0.7, 0.3, and 0.3 ppbv, respectively. In our study, the precision was 0.02 ppbv at 1 Hz.

The detection limits of the EC flux were calculated as the standard deviations of the cross covariances between vertical wind fluctuations and gas concentration fluctuations far outside of the true time lag ($-200\,s \le \tau \le -50\,s$, and $50\,s \le \tau \le 200\,s$) (Neftel et al., 2010, Wienhold et al., 1995). Thus the EC detection limit derived from this method was not a constant value and was dependent on the instruments and atmospheric conditions. The mean detection limit in this study was 2.10 $ng\,N\,m^{-2}\,s^{-1}$, which was less than half of the N_2O flux detection limit of 4.76 $ng\,N\,m^{-2}\,s^{-1}$ as reported in Neftel et al. (2010) and 6.00 $ng\,N\,m^{-2}\,s^{-1}$ in Kroon et al. (2007).

ACPD
14, 20417–20460, 2014

It has been shown that the sensible heat cospectrum calculated from sonic temperatures experiences almost no damping (Neftel et al., 2010; Kroon et al., 2007) (Fig. 4a and b). Therefore an empirical correction approach can be used, based on a comparison of the sensible heat cospectrum and N_2O cospectrum to correct the high frequency loss (Neftel et al., 2010; Kroon et al., 2007). In this study at the low frequency range, the analytic correction procedure proposed by Moncrieff et al. (2004) was used, and at the high frequency range the spectral loss was corrected using the methods of Ibrom et al. (2007) and Horst and Lenschow (2009) in EddyPro 3.0.

Neftel et al. (2010), under a wind speed of 0.8 to 2 $m\,s^{-1}$, reported a 14 to 30 % frequency loss correction ratio compared to a mean correction ratio of 16 % by EddyPro in this study (corresponding to $u^* = 0.2$ to 0.5 $m\,s^{-1}$). Neftel et al. (2010) used a vapor cospectra to correct the frequency loss, whereas, this study used the methods in Ibrom et al. (2007), Horst and Lenschow (2009), and Moncrieff et al. (2004), which may account for the difference in frequency loss correction ratios.

About 93 % of the valid data ($u^* \geq 0.2\,m\,s^{-1}$) in this study were under wind conditions of $0.4\,m\,s^{-1} > u^* \geq 0.2\,m\,s^{-1}$ and were in the daytime, when the corresponding mean frequency loss ratio was low, between 2 and 4 %. Therefore, the flux may have been overestimated because the mean frequency correction ratio was 16–18 % (Table 2).

The mean of the positive frequency loss ratios was greater than 22 % and the mean of the negative loss ratios was smaller than −37 % (for $u^* \geq 0.2\,m\,s^{-1}$) (Table 2). The negative and the positive ratios cancelled out each other and resulted in the mean 2–4 % frequency loss ratios. Therefore, for long-term N_2O flux measurements, the mean frequency loss may be low.

4.2 N_2O emission compared with the literature

A number of studies have been carried out to investigate N_2O emissions from soil to the atmosphere, and the results reported in the literature show tremendous variation (Table 6). Previous studies have shown that the N_2O emission depends on several factors, including precipitation, fertilization, tillage, crop type, soil factor, and instrumenta-

Discussion Paper | Discussion Paper | Discussion Paper | Discussion Paper |

ACPD

14, 20417–20460, 2014

Nitrous oxide emissions from a commercial cornfield

H. Huang et al.

tion (Ussiri et al., 2009; Wagner-Riddle et al., 2007). Fertilizer application was a prime factor causing a different N_2O emission in previous studies. Generally, the measured flux and cumulative emission were larger with a larger amount of fertilizer application (Table 6). In order to obtain a gross synthesization of these previous studies, shown in Table 6, and how this study fits into them, we plotted those which reported both fertilizer applied and the integrated amount of N_2O emissions. Figure 10, presents a simple linear plot of emissions (kg N_2O–N ha^{-1}) (Table 6 column 9) as a function of fertilizer applied (kg N ha^{-1}) (Table 6 column 6). The graph demonstrates a general linear trend ($R^2 = 0.48$, $p < 0.001$) of increasing emissions with increased amounts of N fertilizer, without regard to soil moisture, crop type, tillage, crop management, measurement techniques, or length of time of the study. The simple linear regression shows the ratio of N_2O emissions to N fertilizer to be 0.0143. Thus, in general, it appears that 1.43 % of each unit of N fertilizer applied is emitted to the atmosphere as N_2O.

Corn crops were reported in nine of the studies listed in Table 6. They fit the trends described above. Similar amounts of fertilizers were applied in Lee et al. (2009) and Laville et al. (1999) as in this study; and similar orders of N_2O emission were observed in all three. Where lower applications of fertilizer were reported for corn fields (Molodovskaya et al., 2011, Phillips et al., 2009, Ussiri et al., 2009, Wagner-Riddle et al., 2007, and Grant and Pattey, 2003), lower N_2O emissions were measured.

In addition to fertilization, tillage also has played a role in governing N_2O emissions. Lee and colleagues (Lee et al., 2009) showed that with the same amounts of fertilizers for corn, sunflower, and chickpea, different tillage could cause differences in N_2O emissions. And fully tilled fields tended to release less N_2O.

In general, forest N_2O emissions have been lower than those from agriculture, which was probably due to the large amount of fertilizers applied to farmland. For example, compared to the flux rate 257.5 ± 817.7 µg N_2O–N ha^{-1} h^{-1} in this study, Mammarella et al. (2010) measured an average flux of ∼ 10 µg N_2O–N m^{-2} h^{-1} during 2 May to 5 June 2003 in a beech forest of Denmark. They showed ∼ 5 µg N_2O–N m^{-2} h^{-1} flux during the spring of 2007 in a forest with pine, small-sized spruce, and birch in southern

ACPD
14, 20417–20460, 2014

Finland, using both the EC and chamber methods. Eugster et al. (2007) measured N_2O from a forest mixed with beech and spruce using the EC method. The reported flux was $22.4 \pm 11.2\,\mu g\,N_2O–N\,m^{-2}\,h^{-1}$.

4.3 Effects of soil moisture, temperature, and N availability on N emissions

Soil moisture is a major factor for N_2O emissions (Table 4). As indicated by Dobbie and Smith (2003) and Davidson (1991), N_2O emitted from soil is caused principally by the microbial nitrogen transformations during both nitrification and denitrification. These processes are closely related to WFPS since denitrification is an anaerobic process, which depends on the balance between the amounts of water entering and leaving the soil. Several studies have confirmed that there are connections between increased N_2O emissions and precipitation (Zona et al., 2011; Jungkunst et al., 2008; Neftel et al., 2007, e.g.). In this study, after the first application of fertilizer, precipitation did not occur immediately and there was no significant change of N_2O flux. On the day of the second application, the total precipitation was 3.02 mm and peak values of N_2O fluxes occurred immediately after the precipitation event (Fig. 5). Monitoring these events better captured the trigger effect of precipitation on the N_2O emission. The other notable feature of Fig. 5 was the remarkable increases of N_2O for the days with precipitation. The variations in the increases were apparently caused by the changes in soil moisture content due to precipitation.

During the whole season, soil temperature was not positively related to N_2O flux ($r = -0.084$, $p < 0.01$). Apparently soil temperature generally increased with time during the season, while the N_2O flux did not. Therefore the N_2O flux was correlated mainly with soil moisture (Fig. 9 and Table 4). Thus compared to the factors of soil moisture and N availability, soil temperature had rather weak effects on N_2O emissions at this specific site (Table 4).

However, during the diurnal cycles, when soil moisture was not a predominant factor ($r_{sm} < 0.4$, $p > 0.05$ in the first and second sub-periods), soil temperature was significantly and positively correlated to N_2O emissions ($r_{sm} \geq 0.56$, $p < 0.001$) (Fig. 7). This

ACPD
14, 20417–20460, 2014

indicates if soil moisture is not changed and other factors remain constant, the N_2O emission during the daytime is higher than during the night time. This was likely the reason that the average daytime fluxes were much higher than the night time N_2O fluxes during the whole season: 278.8 ± 865.8 vs. $100.0 \pm 210.0\,\mu g\,N_2O{-}N\,m^{-2}\,h^{-1}$. The soil microorganisms were more active during the warmer daytime and produced more N_2O emissions, as pointed out in Maljanen et al. (2002).

As expected, mineral nitrogen availability was an important factor in N_2O emissions. The fertilizer applications before June may have caused higher soil N availabilities and higher N_2O concentrations than after June (Fig. 6). The fertilizer amount of the second application was more than twice that of the first application; it most likely contributed to the dramatic increase in N_2O concentration and flux after the second application (Fig. 5).

4.4 Response of N_2O emission to precipitation

Soil moisture was strongly dependent on precipitation events. For most precipitation events during the experimental period, the sonic anemometer sensor heads were wet and could not measure the instantaneous wind velocities precisely. Consequently, estimates of the reaction time of emissions to precipitation are lacking. However, there were two events with low rainfall amounts (< 5 mm for each 30 min measurement period), when the sensor heads were not affected (the diagnostic record from the datalogger showed the instruments functioned normally). During these the N_2O emissions increased within 30 min after rainfall, indicating soil N_2O emission likely responds to rainfall and a change of soil moisture very quickly, as noted previously by Phillips et al. (2013) using dynamic chambers. Large emissions immediately after rain events have been shown in emission studies of other gases and vapors, for example, the emissions of mercury have been attributed to the evacuation of high concentration gas in soil pores as they fill up with water (Bash and Miller, 2009; Gillis and Miller, 2000). The same mechanism may be occurring here. In any case, further examination is necessary because the spikes are large and significant emissions during active rainfall may be missed in this and most other field studies.

5 Conclusions

A new N_2O analyzer was operated continuously for EC flux measurements of N_2O in a cornfield in Nolensville, TN, during the period of 4 April–8 August 2012. Based on Allan variance analysis, the precision of the instrument was 0.066 ppbv for 10 Hz measurements. The seasonal mean detection limit of the N_2O flux measurements was 2.10 ng N m^{-2} s^{-1}. The mean frequency loss ratio of the flux measurements was between 0.02(± 1.54) to 0.04(± 0.55) under the conditions of 0.4 m s^{-1} > u^* ≥ 0.2 m s^{-1} during the day and 0.42 ± 0.27 under the conditions of 0.3 m s^{-1} > u^* ≥ 0.2 m s^{-1} during the night. We conclude that this N_2O EC system can be used to provide reliable N_2O flux measurements.

The cumulative N_2O emission from the experimental site during the entire growing season was 6.87 kg N_2O–N ha^{-1}. This study showed that in addition to N availability in soil, the seasonal and diurnal N_2O emission was highly dependent on soil moisture, and extremely high fluxes appeared after a N fertilization event combined with precipitation. Soil moisture variation was a dominant factor affecting N_2O emissions compared to soil temperature, although a diurnal variation in flux was in response to the diurnal soil temperature wave. Average daytime emissions were much higher than night emissions (278.8 vs. 100.0 µg N_2O–N m^{-2} h^{-1}).

Combining these results with 9 previous studies in the literature allowed some preliminary synthesization. It appears that approximately 1.43 % of each unit of N fertilizer was emitted to the atmosphere as N_2O.

ACPD
14, 20417–20460, 2014

6 Future research

We recommend that future studies focus on developing precision methods of minimizing N_2O emissions by careful spatial and temporal control of fertilization amounts, water availability, and tilling practices. These should include "mechanism" studies quantifying the N_2O flux rates from various interactions of water and N levels in soils. The effects of reducing the episodic nature of fertilization and water availability should be quantified and methods developed to make such reductions. Complete field-scale experiments designed to test application rates and application timing and yields will likely produce more usable results than even complete monitoring of commercial field operations.

Acknowledgements. The authors gratefully acknowledge financial support for this research from USDA – Capacity Building Grant (2011-38821-30971), Evans–Allen Grant, and the support from the Illinois State Water Survey at the University of Illinois at Urbana-Champaign. The authors thank Roger Sauve (Tennessee State University) for helping arrange the commercial farm for the experiment. We also thank Eddie Williams, Daniel Doss, and Emeka Nwaneri for field experimental assistance. Opinions expressed are those of the authors and not necessarily those of the Illinois State Water Survey, the Prairie Research Institute, or the University of Illinois.

References

Arnold, K., Nilsson, M., Hanell, B., Weslien, P., and Klemedtsson, L.: Fluxes of CO_2, CH_4 and N_2O from drained organic soils in deciduous forests, Soil Biol. Biochem., 37, 1059–1071, 2005.

Aubinet, M., Grelle, A., Ibrom, A., Rannik, Ü., Moncrieff, J., Foken, T., Kowalski, A. S., Martin, P. H., Berbigier, P., Bernhofer, C., Clement, R., Elbers, J., Granier, A., Grünwald, T., Morgenstern, K., Pilegaard, K., Rebmann, C., Snijders, W., Valentini, R., and Vesala, T.: Estimates of the annual net carbon and water exchange of European forests: the EUROFLUX methodology, Adv. Ecol. Res., 30, 113–173, 2000.

Bash, J. O. and Miller, D. R.: Growing season total gaseous mercury (TGM) flux measurements over an acer rubrum forest, Atmos. Environ., 43, 5953–5961, 2009.

Bouwman, A. F.: Direct emission of nitrous oxide from agricultural soils, Nutr. Cycl. Agroecosys., 46, 53–70, 1996.
Bouwman, A. F, Boumans, L., and Batjes, N. H.: Emissions of N_2O and NO from fertilized fields: summary of available measurement data, Global Biogeochem. Cy., 16, 1–13, 2002.
Davidson, E. A.: Fluxes of nitrous oxide and nitric oxide from terrestrial ecosystems, in: Microbial production and consumption of greenhouse gases: methane, nitrogen oxides, and halomethanes, American Society for Microbiology, Washington, DC, 219–235, 1991
Davidson, E. A. and Swank, W. T.: Environmental parameters regulating gaseous nitrogen losses from two forested ecosystems via nitrification and denitrification, Appl. Environ. Microb., 52, 1287–1292, 1986.
Denmead, O. T.: Approaches to measuring fluxes of methane and nitrous oxide between landscapes and the atmosphere, Plant Soil, 309, 5–24, 2008.
Dinsmore, K. J., Skiba, U. M., Billett, M. F., Rees, R. M., and Drewer, J.: Spatial and temporal variability in CH_4 and N_2O fluxes from a Scottish ombrotrophic peatland: implications for modelling and up-scaling, Soil Biol. Biochem., 6, 1315–1323, 2009.
Dobbie, K. E. and Smith, K. A.: Nitrous oxide emission factors for agricultural soils in Great Britain: the impact of soil water-filled pore space and other controlling variables, Glob. Change Biol., 9, 204–218, 2003.
Eddypro Version 3.0: Eddypro Version 3.0 User's Guide &, LI-COR, Inc., Lincoln, NE 68504-0425, 2012.
Edwards, G. C., Thurtell, G. W., Kidd, G. E., Dias, G. M., and Wagner-Riddle, C.: A diode laser based gas monitor suitable for measurement of trace gas exchange using micrometeorological technique, Agr. Forest Meteorol., 115, 71–89, 2003.
Eugster, W., Zeyer, K., Zeeman, M., Michna, P., Zingg, A., Buchmann, N., and Emmenegger, L.: Methodical study of nitrous oxide eddy covariance measurements using quantum cascade laser spectrometery over a Swiss forest, Biogeosciences, 4, 927–939, doi:10.5194/bg-4-927-2007, 2007.
Famulari, D., Nemitz, E., Marco, C. D., Phillips, G. J., Thomas, R., House, E., and Fowler, D.: Eddy-covariance measurements of nitrous oxide fluxes above a city, Agr. Forest Meteorol., 150, 786–793, 2010.
Ferrara, R. M., Loubet, B., Tommasi, P. D., Bertolini, T., Magliulo, V., Cellier, P., Eugster, W., and Rana, G.: Eddy covariance measurement of ammonia fluxes: comparison of high frequency correction methodologies, Agr. Forest Meteorol., 158–159, 30–42, 2012.

Forster, P., Ramaswamy, V., Artaxo, P., Berntsen, T., Betts, R., Fahey, D. W., Haywood, J., Lean, J., Lowe, D. C., Myhre, G., Nganga, J., Prinn, R., Raga, G., Schulz, M., and Van Dorland, R.: Changes in atmospheric constituents and in radiative forcing, in: Climate Change 2007: The Physical Science Basis. Contribution of Working Group I to the Fourth Assessment Report of the Intergovernmental Panel on Climate Change, Cambridge University Press, Cambridge, Chapt. 2, 2007.

Gillis, A. A. and Miller, D. R.: Some local environmental effects on mercury emission and absorption at a soil surface, Sci. Total Environ., 260, 191–200, 2000.

Grant, R. F. and Pattey, E.: Modelling variability in N_2O emissions from fertilized agricultural fields, Soil Biol. Biochem., 35, 225–243, 2003.

Gu, L., Falge, E. M., Boden, T., Baldocchi, D. D., and Black, T. A.: Objective threshold determination for nighttime eddy flux filtering, Agr. Forest Meteorol., 128, 179–197, 2005.

Halvorson, A. D., Schweissing, F. C., Bartolo, M. E., and Reule, C. A.: Corn response to nitrogen fertilization in a soil with high residual nitrogen, Agron. J., 97, 1222–1229, 2005.

Horst, T. W. and Lenschow, D. H.: Attenuation of scalar fluxes measured with spatially-displaced sensors, Bound.-Lay. Meteorol., 130, 275–300, 2009.

Ibrom, A., Dellwik, E., Larse, S. E., and Pilegaard, K.: On the use of the Webb–Pearman–Leuning theory for closed-path eddy correlation measurements, Tellus B, 59, 937–946, 2007.

Jones, S. K., Famulari, D., Di Marco, C. F., Nemitz, E., Skiba, U. M., Rees, R. M., and Sutton, M. A.: Nitrous oxide emissions from managed grassland: a comparison of eddy covariance and static chamber measurements, Atmos. Meas. Tech., 4, 2179–2194, doi:10.5194/amt-4-2179-2011, 2011.

Jungkunst, H. F., Fless, H., Scherber, C., and Fiedler, S.: Groundwater level controls CO_2, N_2O and CH_4 fluxes of three different hydromorphic soil types of a temperate forest ecosystem, Soil Biol. Biochem., 40, 2047–2057, 2008.

Kaimal, J. C. and Finnigan, J. J.: Atmospheric Boundary Layer Flows, 2nd edn., Oxford University Press, New York, 1994.

Kaimal, J. C., Wyngaard, J. C., Izumi, Y., and Cote, O. R.: Deriving power spectra from a three-component sonic anemometer, J. Appl. Meteorol., 7, 827–837, 1972.

Kitzler, B., Zechmeister-Boltenstern, S., Holtermann, C., Skiba, U., and Butterbach-Bahl, K.: Controls over N_2O, NO_x and CO_2 fluxes in a calcareous mountain forest soil, Biogeosciences, 3, 383–395, doi:10.5194/bg-3-383-2006, 2006.

Klemedtsson, L., Klemedtsson, A. K., Moldan, F., and Weslien, P.: Nitrous oxide emission from Swedish forest soils in relation to liming and simulated increased N-deposition, Biol. Fert. Soils, 25, 290–295, 1996.

Kroeze, C., Mosier, A., and Bouwman, L.: Closing the global warming budget: a retrospective analysis 1500–1994, Global Biogeochem. Cy., 13, 1–8, 1999.

Kroon, P. S., Hensen, A., Jonker, H. J. J., Zahniser, M. S., van't Veen, W. H., and Vermeulen, A. T.: Suitability of quantum cascade laser spectroscopy for CH_4 and N_2O eddy covariance flux measurements, Biogeosciences, 4, 715–728, doi:10.5194/bg-4-715-2007, 2007.

Laville, P., Jambert, C., Cellier, P., and Delmas, R.: Nitrous oxide fluxes from a fertilized maize crop using micrometeorological and chamber methods, Agr. Forest Meteorol., 96, 19–38, 1999.

Lee, J., Hopmans, J. W., Kessel., C., King, A. P., Evatt., K. J., Louie, D., Rolston, D. E., and Six, J.: Tillage and seasonal emissions of CO_2, N_2O and NO across a seed bed and at the field scale in a Mediterranean climate, Agr. Ecosyst. Environ., 129, 378–390, 2009.

Li, J., Tong, X., Yu, Q., Dong, Y., and Peng, C.: Micrometeorological measurements of nitrous oxide exchange in a cropland, Atmos. Environ., 42, 6992–7001, 2008.

Liu, C., Wang, K., and Zheng, X.: Responses of N_2O and CH_4 fluxes to fertilizer nitrogen addition rates in an irrigated wheat-maize cropping system in northern China, Biogeosciences, 9, 839–850, doi:10.5194/bg-9-839-2012, 2012.

Luo, G. J., Kiese, R., Wolf, B., and Butterbach-Bahl, K.: Effects of soil temperature and moisture on methane uptake and nitrous oxide emissions across three different ecosystem types, Biogeosciences, 10, 3205–3219, doi:10.5194/bg-10-3205-2013, 2013.

Ma, B. L., Wu, T. Y., Tremblay, N., Deen, W., Morrison, M. J., Mclaughlin, N. B., Gregorich, E. G., and Stewart, G.: Nitrous oxide fluxes from corn fields: on-farm assessment of the amount and timing of nitrogen fertilizer, Glob. Change Biol., 16, 156–170, 2010.

Maljanen, M., Martikainen, P. J., Aaltonen, H., and Silvola, J.: Short-term variation in fluxes of carbon dioxide, nitrous oxide and methane in cultivated and forested organic boreal soils, Soil Biol. Biochem., 34, 577–584, 2002.

Mammarella, I.: Lecture 1 EC Method Background and Theory, available at: http://www.abba.ethz.ch/committee/LECTURE_Mammarella.pdf (last access: 31 July 2014), ETH Zurich, Zurich, Switzerland, 2011.

ACPD
14, 20417–20460, 2014

Mammarella, I., Werle, P., Pihlatie, M., Eugster, W., Haapanala, S., Kiese, R., Markkanen, T., Rannik, Ü., and Vesala, T.: A case study of eddy covariance flux of N_2O measured within forest ecosystems: quality control and flux error analysis, Biogeosciences, 7, 427–440, doi:10.5194/bg-7-427-2010, 2010.
Marco, C. D., Skiba, U., Weston, K., Hargreaves, K., and Fowler, D.: Field scale N_2O flux measurements from grassland using eddy covariance, Water Air Soil Poll., 4, 143–149, 2004.
Molodovskaya, M., Warland, J., Richards, B. K., Oberg, G., and Steenhuis, T. S.: Nitrous oxide from heterogeneous agricultural landscapes: source contribution analysis by eddy covariance and chambers, Soil Sci. Soc. Am. J., 75, 1829–1838, 2011.
Moncrieff, J., Clement, R., Finnigan, J., and Meyers, T.: Averaging, Detrending, and Filtering of Eddy Covariance Time Series, Vol. 29, Chapt. 2, Kluwer Academic Publishers, Dordrecht, Netherlands, 7–31, 2004.
Mosier, A., C., Kroeze, Nevison, C., Oenema, O., Seitzinger, S., and Cleemput, O.: Closing the global N_2O budget: nitrous oxide emissions through the agricultural nitrogen cycleOECD/IPCC/IEA phase II development of IPCC guidelines for national greenhouse gas inventory methodology, Nutr. Cycl. Agroecosys., 52, 225–248, 1998.
Neftel, A., Flechard, C. R., Ammann, C., Conen, F., Emmenegger, L., and Zeyer, K.: Experimental assessment of N_2O background fluxes in grassland systems, Tellus B, 59, 470–482, 2007.
Neftel, A., Ammann, C., Fischer, C., Spirig, C., Conen, F., Emmenegger, L., Tuzson, B., and Wahlen, S.: N_2O exchange over managed grassland: application of a quantum cascade laser spectrometer for micrometeorological flux measurements, Agr. Forest Meteorol., 150, 775–785, 2010.
Nelson, D.: TDLWintel User's Manual,Aerodyne Research, Inc, Billerica, MA, USA, 2002.
Nelson, D. D., McManus, B., Urbanski, S., Herndon, S., and Zahniser, M. S.: High precision measurements of atmospheric nitrous oxide and methane using thermoelectrically cooled mid-infrared quantum cascade lasers and detectors, Spectrochim. Acta A, 60, 3325–3335, 2004.
Papale, D., Reichstein, M., Aubinet, M., Canfora, E., Bernhofer, C., Kutsch, W., Longdoz, B., Rambal, S., Valentini, R., Vesala, T., and Yakir, D.: Towards a standardized processing of Net Ecosystem Exchange measured with eddy covariance technique: algorithms and uncertainty estimation, Biogeosciences, 3, 571–583, doi:10.5194/bg-3-571-2006, 2006.

ACPD
14, 20417–20460, 2014

Nitrous oxide emissions from a commercial cornfield

H. Huang et al.

Phillips, R. L., Tanaka, D. L., Archer, D. W., and Hanson, J. D.: Fertilizer application timing influences greenhouse gas fluxes over a growing season, J. Environ. Qual., 28, 1569–1579, 2009.
Phillips, R., Griffith, D. W. T., Dijkstra, F.,Lugg, G., Lawrie, R., and Macdonald, B.: Tracking short-term effects of 15N addition on N_2O fluxes using FTIR spectroscopy. J. Environ. Qual. 42, 1327–1340, 2013.
Pihlatie, M., Rinne, J., Ambus, P., Pilegaard, K., Dorsey, J. R., Rannik, Ü., Markkanen, T., Launiainen, S., and Vesala, T.: Nitrous oxide emissions from a beech forest floor measured by eddy covariance and soil enclosure techniques, Biogeosciences, 2, 377–387, doi:10.5194/bg-2-377-2005, 2005.
Ravishankara, A. R., Daniel, J. S., and Portmann, R. W.: Nitrous oxide (N_2O): the dominant ozone-depleting substance emitted in the 21st century, Science, 326, 123–125, 2009.
Saleska, S. R., Miller, S. D., Matross, D. M., Goulden, M. L.,Wofsy, S. C., da Rocha, H. R., de Camargo, P. B., Crill, P., Daube, B. C., de Freitas, H. C., Hutyra, L., Keller, M., Kirchhoff, V., Menton, M., Munger, J. W., Pyle, E. H., Rice, A. H., and Silva, H.: Carbon in Amazon forests: unexpected seasonal fluxes and disturbance-induced losses, Science, 302, 1554–1557, 2003.
Schindlbacher, A., Zechmeister-Boltenstern, S., and Butterbach-Bahl, K.: Effects of soil moisture and temperature on NO, NO_2, and N_2O emissions from European forest soils, J. Geophys. Res., 109, D17302, doi:10.1029/2004JD004590, 2004.
Simpson, I. J., Edwards, G. C., Thurtell, G. W., den Hartog, G., Neumann, H. H., and Staebler, R. M.: Micrometeorological measurements of methane and nitrous oxide exchange above a boreal aspen forest, J. Geophys. Res., 102, 29331–29341, 1997.
Smith, K. A., Ball, T., Conen, F., Dobbie, K. E., Massheder, J., and Rey, A.: Exchange of greenhouse gases between soil and atmosphere: interactions of soil physical factors and biological processes, Eur. J. Soil Sci., 54, 779–791, 2003.
Stull, R. B.: An Introduction to Boundary Layer Meteorology, Kluwer Academic Publishers, Dordrecht, 1988.
Tao, L., Sun, K., Buglione, J., and Zondlo, M.: Flux chamber measurements of nitrous oxide emission at Wetlands, available at: http://meri.njmeadowlands.gov/projects/flux-chamber-measurements-of-nitrous-oxide-emission-at-wetlands/ (last access: 31 July 2014), Meadowlands Environmental Research Institute, Lyndhurst, New Jersey, 2013.

Ussiri, D. A. N., Lal, R., and Jarecki, M. K.: Nitrous oxide and methane emissions from long-term tillage under a continuous corn cropping system in Ohio, Soil Till. Res., 104, 247–255, 2009.
Vickers, D. and Mahrt, L.: Quality control and flux sampling problems for tower and aircraft data, J. Atmos Ocean. Tech., 14, 512–526, 1997.
Wagner-Riddle, C., Furon, A., McLaughlin, N. L., Lee, I., Barbeau, J., Jayasundara, S., Parkin, G., Von Bertoldi, P., and Warland, J.: Intensive measurement of nitrous oxide emissions from a corn-soybean-wheat rotation under two contrasting management systems over 5 years, Glob. Change Biol., 8, 1722–1736, 2007.
Wang, K, Zheng, X., Pihlatie, M., Vesala, T., Liu, C., Haapanala, S., Mammarella, I., Rannik, Ü., and Liu, H.: Comparison between static chamber and tunable diode laser-based eddy covariance techniques for measuring nitrous oxide fluxes from a cotton field, Agr. Forest Meteorol., 171–172, 9–19, 2013.
Wienhold, F. G., Welling, M., and Harris, G. W.: Micrometeorological measurements and source region analysis of nitrous oxide fluxes from an agricultural soil, Atmos. Environ., 29, 2219–2227, 1995.
Zona, D., Janssens, I. A., Verlinden, M. S., Broeckx, L. S., Cools, J., Gioli, B., Zaldei, A., and Ceulemans, R.: Impact of extreme precipitation and water table change on N_2O fluxes in a bio-energy poplar plantation, Biogeosciences Discuss., 8, 2057–2092, doi:10.5194/bgd-8-2057-2011, 2011.
Zou, J, Huang, Y., Lu, Y., Zheng, X., and Wang, Y.: Direct emission factor for N_2O from rice–winter wheat rotation systems in southeast China, Atmos. Environ., 39, 4755–4765, 2005.

ACPD
14, 20417–20460, 2014

Table 1. Overview of four measurement periods characterized by precipitation and fertilization. Two fertilizer application events were on 10 April and 14 May 2012 respectively. Before the experiment 99 $\mathrm{kg\,N\,ha^{-1}}$ chicken litter was applied on 10 March, total precipitation was calculated as the sum of precipitation of each period.

Index	Date	Fertilization $\mathrm{kg\,N\,ha^{-1}}$	Total precipitation (mm)
S1D	4–25 Apr, day	39 (URAN-32-0-0)	15.73
S1N	4–25 Apr, night	–	28.68
S2D	26 Apr–26 May, day	79 (URAN-32-0-0)	69.82
S2N	26 Apr–26 May, night	–	96.23
S3D	27 May–24 Jun, day	–	20.32
S3N	27 May–24 Jun, night	–	8.62
S4D	25 Jun–8 Aug, day	–	74.38
S4N	25 Jun–8 Aug, night	–	53.56

Table 2. Variation of frequency loss ratio $\frac{\Delta\emptyset}{\emptyset}$ and frequency loss correction ratio by EddyPro $\frac{\Delta\emptyset}{\emptyset}$(EP) with friction velocity (u^*, $\mathrm{m\,s^{-1}}$) for May 2012. N/A: not available. Numbers in the cells are mean ± standard deviations.

u^*	$0 \le u^* < 0.1$			$0.1 \le u^* < 0.2$			$0.2 \le u^* < 0.3$		
Rang of Loss ratio	≥ 0	< 0	all	≥ 0	< 0	all	≥ 0	< 0	all
Daytime									
# of samples	16	18	34	84	65	149	113	140	253
$\frac{\Delta\emptyset}{\emptyset}$	0.43 ± 0.48	−0.42 ± 0.48	0.02 ± 0.64	0.33 ± 0.55	−0.45 ± 1.10	0.01 ± 0.91	0.43 ± 1.29	−0.39 ± 1.64	0.02 ± 1.54
$\frac{\Delta\emptyset}{\emptyset}$(EP)	0.16 ± 0.01	0.16 ± 0.01	0.16 ± 0.01	0.16 ± 0.00	0.15 ± 0.00	0.16 ± 0.01	0.16 ± 0.01	0.16 ± 0.01	0.16 ± 0.01
Nighttime									
# of samples	145	91	236	47	12	59	4	N/A	4
$\frac{\Delta\emptyset}{\emptyset}$	0.76 ± 1.35	−0.84 ± 1.66	0.14 ± 1.67	0.90 ± 1.09	−0.23 ± 0.26	0.66 ± 1.08	0.42 ± 0.27	N/A	0.42 ± 0.27
$\frac{\Delta\emptyset}{\emptyset}$(EP)	0.16 ± 0.01	0.16 ± 0.01	0.16 ± 0.01	0.16 ± 0.01	0.16 ± 0.00	0.16 ± 0.01	0.16 ± 0.01	N/A	0.16 ± 0.01

u^*	$0.3 \le u^* < 0.4$			$0.4 \le u^* < 0.5$		
Rang of Loss ratio	≥ 0	< 0	all	≥ 0	< 0	all
Daytime						
# of samples	27	22	49	2	N/A	2
$\frac{\Delta\emptyset}{\emptyset}$	0.22 ± 0.22	−0.37 ± 0.67	0.04 ± 0.55	0.31 ± 0.29	N/A	0.31 ± 0.29
$\frac{\Delta\emptyset}{\emptyset}$(EP)	0.18 ± 0.01	0.17 ± 0.01	0.18 ± 0.01	0.16 ± 0.01	N/A	0.16 ± 0.01
Nighttime						
# of samples	N/A	N/A	N/A	N/A	N/A	N/A
$\frac{\Delta\emptyset}{\emptyset}$	N/A	N/A	N/A	N/A	N/A	N/A
$\frac{\Delta\emptyset}{\emptyset}$(EP)	N/A	N/A	N/A	N/A	N/A	N/A

Discussion Paper | Discussion Paper | Discussion Paper | Discussion Paper |

ACPD

14, 20417–20460, 2014

Nitrous oxide emissions from a commercial cornfield

H. Huang et al.

Table 3. Descriptive statistics for 30 min N_2O concentration and flux for the period of experiment, 4 April-8 August 2012 ($u^* \geq 0.2\,m\,s^{-1}$).

	Number of samples	Concentration (ppbv)				Flux ($\mu g\,N_2O{-}N\,m^{-2}\,h^{-1}$)			
		Mean	Median	Standard deviation	Skewness	Mean	Median	Standard deviation	Skewness
Daytime	1224	322.9	324.5	4.04	0.396	278.8	91.1	865.8	7.075
Nighttime	166	322.5	324.4	3.70	0.009	99.9	45.9	209.9	6.611
Total	1390	322.8	324.5	4.00	0.364	257.5	83.4	817.7	7.482

ACPD
14, 20417–20460, 2014

Nitrous oxide emissions from a commercial cornfield

H. Huang et al.

Table 4. Statistical results of 30 min soil temperature (°C), soil moisture (%) and N_2O flux (µg N_2O–N m^{-2} h^{-1}) (mean ± standard deviation), as well as Pearson correlation coefficients (r) of N_2O flux with soil temperature or soil moisture ($u^* \geq 0.2$ m s^{-1}).

Index	Date	Number of samples	Soil temperature	Soil moisture	Flux	Soil temperature *r* (p)	Soil moisture *r* (p)
S1D	4–25 Apr, day	274	18.0 ± 3.0	11.8 ± 2.9	172.7 ± 236.0	0.175 (0.003)	0.606 (0.000)
S1N	4–25 Apr, night	48	18.9 ± 2.3	12.1 ± 3.2	62.7 ± 72.8	0.449 (0.001)	0.067 (0.653)
S2D	26 Apr–26 May, day	392	23.0 ± 2.6	15.0 ± 4.3	603.2 ± 1448.5	−0.195 (0.000)	0.488 (0.000)
S2N	26 Apr–26 May, night	35	21.9 ± 2.8	12.0 ± 3.3	173.7 ± 215.0	0.496 (0.002)	0.644 (0.000)
S3D	27 May–24 Jun, day	326	24.9 ± 2.2	11.1 ± 4.6	60.2 ± 51.3	−0.192 (0.000)	0.780 (0.000)
S3N	27 May–24 Jun, night	36	26.8 ± 2.4	12.0 ± 5.2	88.4 ± 156.6	0.149 (0.385)	0.605 (0.000)
S4D	25 Jun–8 Aug, day	232	27.1 ± 1.6	10.5 ± 4.2	162.4 ± 273.6	−0.245 (0.000)	0.571 (0.000)
S4N	25 Jun–8 Aug, night	47	28.8 ± 1.2	8.2 ± 4.1	92.1 ± 306.8	−0.491 (0.000)	0.526 (0.000)
Whole experimental period, day		1224	23.2 ± 4.0	12.4 ± 4.5	278.8 ± 865.8	−0.084 (0.003)	0.424 (0.000)
Whole experimental period, night		166	23.9 ± 4.5	10.2 ± 4.0	100.0 ± 210.0	0.045 (0.560)	0.500 (0.000)

ACPD
14, 20417–20460, 2014

ACPD
14, 20417–20460, 2014

Nitrous oxide emissions from a commercial cornfield

H. Huang et al.

Table 5. Thirty min N_2O flux (µg $N_2O{-}N\,m^{-2}\,h^{-1}$) regression equations ($p < 0.01$) with soil moisture (SM, %) and soil temperature (ST, °C) ($u^* \geq 0.2\,m\,s^{-1}$).

Date	Day equation	R^2	Night equation	R^2
4–25 Apr	$20.16e^{19.398SM}$	0.45	$-137.736 + 5.6448SM + 564.48ST$	0.62
26 Apr–26 May	$209037600SM^4 - 11612160SM^3 + 2360304SM^2 - 191720SM + 66185.28$	0.68	$18e^{16.479SM}$	0.45
27 May–24 Jun	$66154.68SM^3 - 137696.28SM^2 + 967.68SM + 10.08$	0.71	$6.048e^{16.308SM}$	0.70
25 Jun–8 Aug	$20.16e^{18.349SM}$	0.54	$0.5e^{23.113SM}$	0.54

Table 6. Summary of N_2O measurements in literature (mean flux (or flux range) and cumulative emission), EC indicates eddy covariance method, "–" indicates data or information is not available directly from the reference.

Reference	Location	Period	Plant	Tillage	Fertilizer, $kg\,N\,ha^{-1}$	Method	Flux, $\mu g\,N_2O{-}N\,m^{-2}\,h^{-1}$	Cumulative emission, $kg\,N_2O{-}N\,ha^{-1}$
this study	Williamson, USA	Apr–Aug 2012	Corn	No till	217	EC	257.5 ± 817.7	6.9
Wang et al. (2013)	Shanxi, China	Jan–Oct 2009	Cotton	Till	75	Chamber	1.2–468.8	1.43
		Jan–Dec 2009	Cotton	Till	75	EC	−10.8–912.0	3.15
Molodovskaya et al. (2011)	Hardford, New York	Jun–Jul 2008	Corn	Till	125	Chamber	30.0 ± 48.0	–
			Alfalfa	Till	750	Chamber	66.0 ± 42.0	–
			Between corn and Alfalfa	–	–	EC	78.0 ± 420.0	
Neftel et al. (2010)	central Swiss	Jun–Sep 2008	Grass	Till	230	Chamber	121.0	3.1
						EC	56.5	1.5[a]
Mammarella et al. (2010)	Sorø, Denmark	May 2003	Beech	–	–	Chamber	9.9 ± 0.12	–
						EC	7.2 ± 0.40	–
	Kalevansuo, Finland	Apr–Jun 2007	Pine, spruce, birch	–	–	Chamber	4.5 ± 0.03	–
						EC	4.6 ± 1.0	–
Lee et al. (2009)	Yolo, California	Apr–Sep 2004	Corn	Standard till	244	Chamber	0–100.8[a]	3.8
				minimum tillage	244	Chamber	0–412.0[a]	8.5
Phillips et al. (2009)	Mandan, North Dakota	Apr–Aug 2008	Corn	No till	70 (early spring)	Chamber	210.0[b]	0.6 ± 0.31
					70 (late spring)	Chamber	270.0[b]	0.7 ± 0.22
Ussiri et al. (2009)	Clarleston, USA	Nov 2004–Nov 2005	Corn	No till	200	Chamber	12.1	0.9
				Chisel till	200	Chamber	30.8	2.0
				Moldboard till	200	Chamber	27.9	1.8
Li et al. (2008)	Luancheng China	1995–1998	Corn		320.5	Gradient	−4410.0–4840.0	–
			Wheat	–	247	Gradient	−2820.0–3590.0	–
Eugster et al. (2007)	Lägeren mountain, Switzerland	Oct–Nov 2005	Beech, spruce	–	–	EC	22.4 ± 11.2	–
Kroon et al. (2007)	Reeuwijk, the Netherlands	Aug–Nov 2006	Grass	–	337	EC	187.2 ± 284.4	–
Wagner-Riddle et al. (2007)	Ontario, Canada	2000–2001	Corn	Till	150	Gradient	24.0[c]	1.2 ± 0.08
				No till	110	Gradient	17.8[c]	1.0 ± 0.07

ACPD
14, 20417–20460, 2014

Nitrous oxide emissions from a commercial cornfield

H. Huang et al.

Table 6. Continued.

Reference	Location	Period	Plant	Tillage	Fertilizer, kg N ha^{-1}	Method	Flux, µg N_2O–N m^{-2} h^{-1}	Cumulative emission, kg N_2O–N ha^{-1}
		2001–2002	Soybean	Till	–	Gradient	15.0[c]	0.7 ± 0.06
				No till	–	Gradient	10.0[c]	0.5 ± 0.01
		2002–2003	Wheat	Till	90	Gradient	17.4[c]	3.0 ± 0.39
				No till	60	Gradient	8.1[c]	0.7 ± 0.11
		2003–2004	Corn	Till	150	Gradient	39.1[c]	1.8 ± 0.20
				No till	110	Gradient	10.1[c]	1.6 ± 0.16
		2004–2005	Soybean	Till	–	Gradient	5.9c	0.3 ± 0.08
				No till	–	Gradient	3.6[c]	0.3 ± 0.01
Kitzler et al. (2006)	North Tyrol Limestone Alps, Austria	May 2002–Apr 2003	Spruce, fir, beech	–	–	Chamber	4.5	0.3 ± 0.11
		May 2003–Apr 2004	Spruce, fir, beech	–	–	Chamber	4.4	0.4 ± 0.09
Zou et al. (2005)	Nanjing, China	May 2002–Oct 2002	Rice	–	0	Chamber	48.2	1.38 ± 0.01
					150	chamber	100.0[a]	2.67 ± 0.07
					300	chamber	170.0[a]	4.44 ± 0.16
					450	chamber	215.9	6.17 ± 0.42
		Nov 2002–Jun 2003	Winter wheat	–	0	chamber	53.8	2.84 ± 0.03
					100	chamber	91.5	4.83 ± 0.06
					200	chamber	110.0[a]	6.44 ± 0.08
					300	chamber	137.8	7.27 ± 0.43
Grant and Pattey (2003)	Ottawa, Canada	May–Jul 1998	Corn	Till	155	EC	–	2.2
					99	EC	–	1.2
Laville et al. (1999)	Landes de Gascogne, France	Jun 1999	Corn	Till	200	Chamber	90–990	–
						EC	72–1440	–
Simpson et al. (1997)	Saskatehewan, Canada	Apr–Sep 1994	Aspen	–	–	Gradient	5.04 ± 2.5	–

[a] Values are not given directly, calculated from known variables.
[b] The measurements were taken at 1000–1200 h daily, and used as the daily flux.
[c] Median, instead of mean.

ACPD
14, 20417–20460, 2014

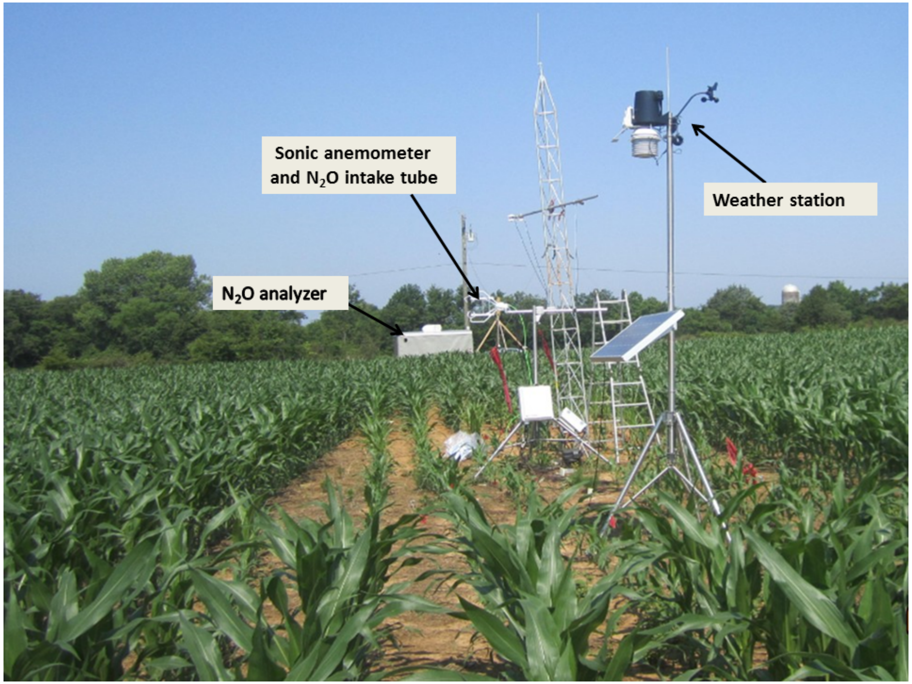

Figure 1. Photo of the experimental site, Williamson County (Nolensville, TN).

ACPD
14, 20417–20460, 2014

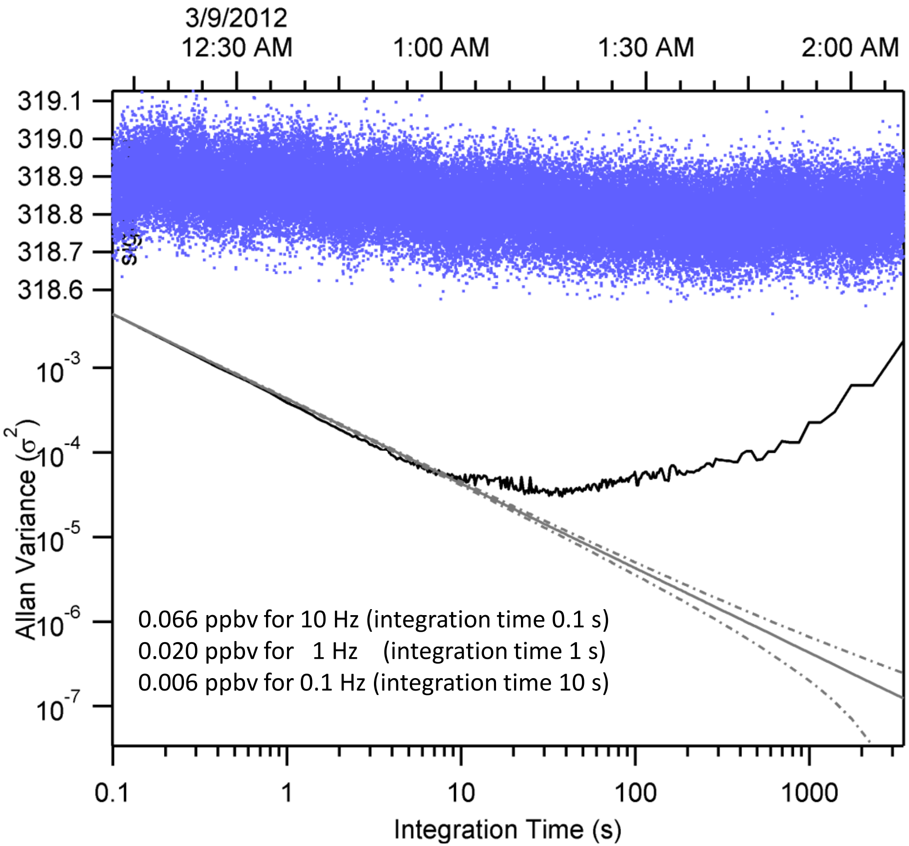

Figure 2. Time series of measured N_2O concentrations (blue dots, ppbv, 10 Hz) under field conditions and the associated Allan variance, downward sloping straight line shows the theoretical behavior of white noise (with a slope of −1, bracketed by dot dash lines showing the 95 % confidence interval), provided by Mark Zahniser at Aerodyn.

ACPD
14, 20417–20460, 2014

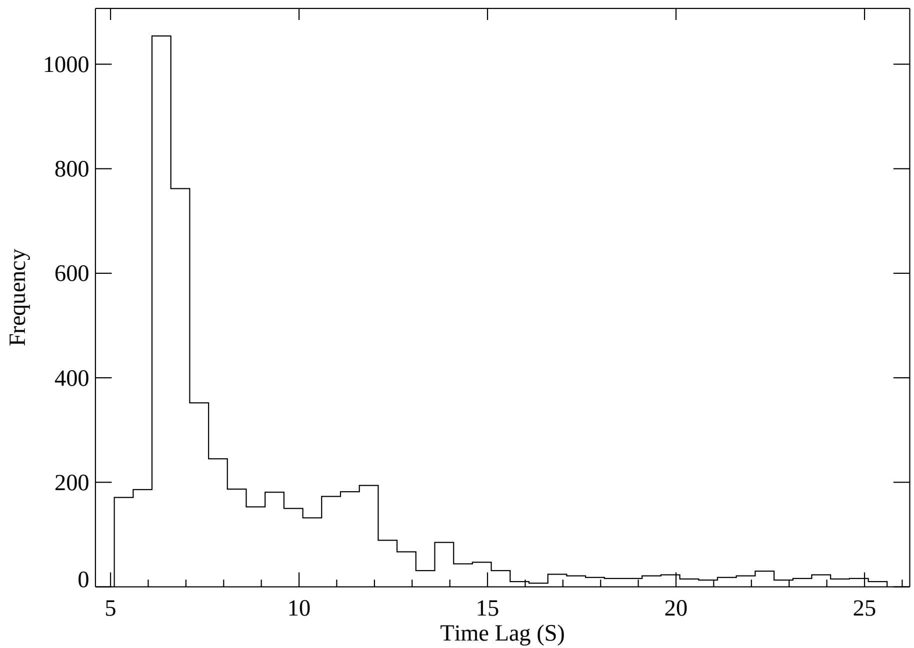

Figure 3. Whole-season histogram of the frequency distribution of time lags of N_2O measurements from wind velocity measurements, found by searching the maximum of cross-covariance.

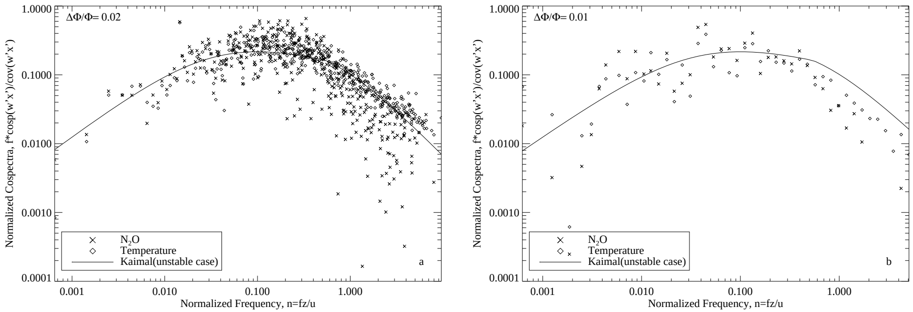

Figure 4. Normalized cospecta, **(a)** daytime (7 a.m. to 7 p.m. 22 May 2012, $u^* \geq 0.2$, $L < 0$), **(b)** night time (7 p.m. 16 May to 7 a.m. 17 May 2012, $u^* \geq 0.2$, $L < 0$). (L is the stability parameter: Obuckov Length (m) outputted from Eddypro; because under stable conditions ($L > 0$), the eddies may not have been well developed, the nighttime unstable conditions ($L < 0$) were chosen.) The axis is normalized frequency, $n = fz/u$, f is natural frequency (Hz); z is measuring height (m); and u is wind speed ($\mathrm{m\,s^{-1}}$). The idealized undamped cospectrum according to Kaimal et al. (1972) and sensible heat cospectrum are also given.

ACPD
14, 20417–20460, 2014

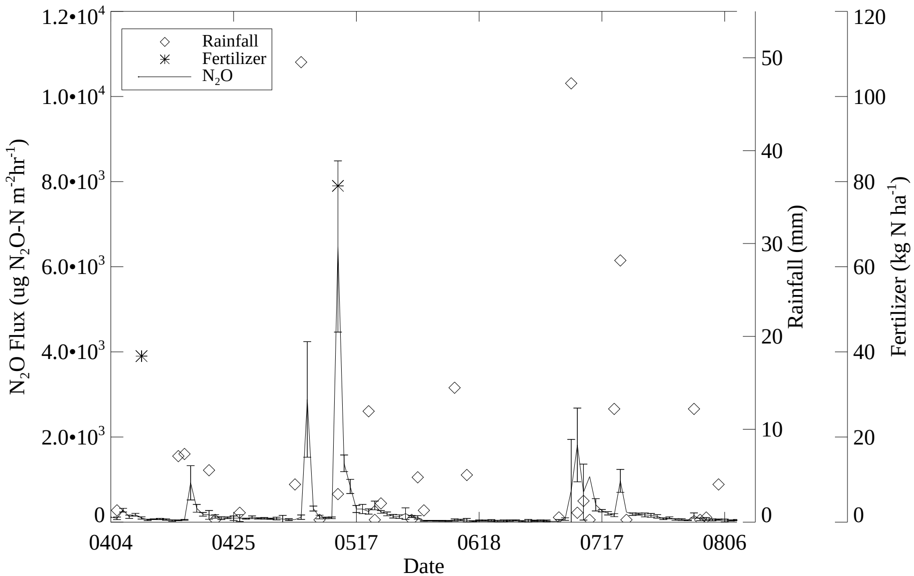

Figure 5. Daily average N_2O flux ($\mu g\, N_2O{-}N\, m^{-2}\, h^{-1}$) with rainfall and N fertilizer applications from 4 April to 8 August 2012. Error bars were the standard deviations of all data collected on each day ($u^* \geq 0.2\, m\, s^{-1}$).

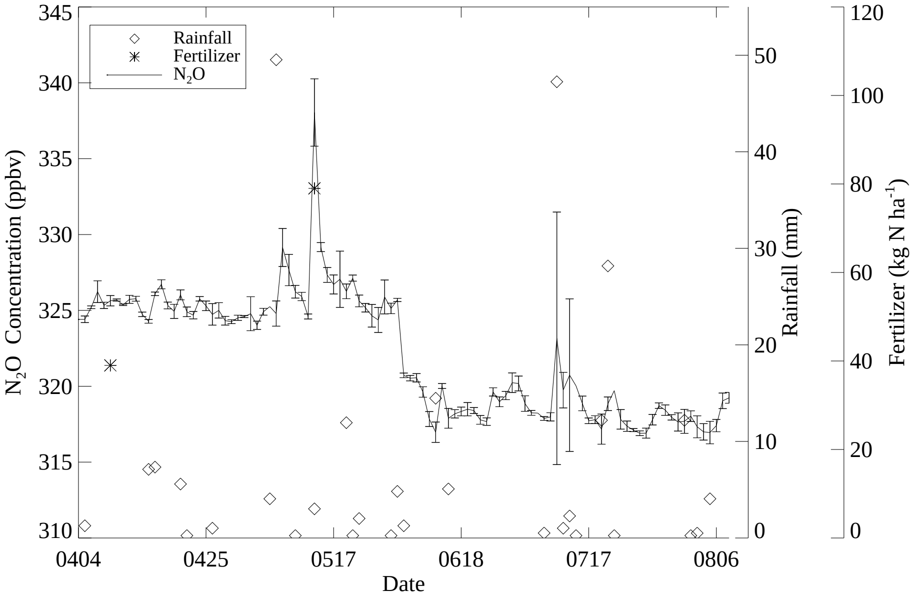

Figure 6. Daily average N_2O concentration (ppbv) with rainfall and N fertilizer applications from 4 April to 8 August 2012. Error bars were the standard deviations of all data collected on each day ($u^* \geq 0.2\,m\,s^{-1}$).

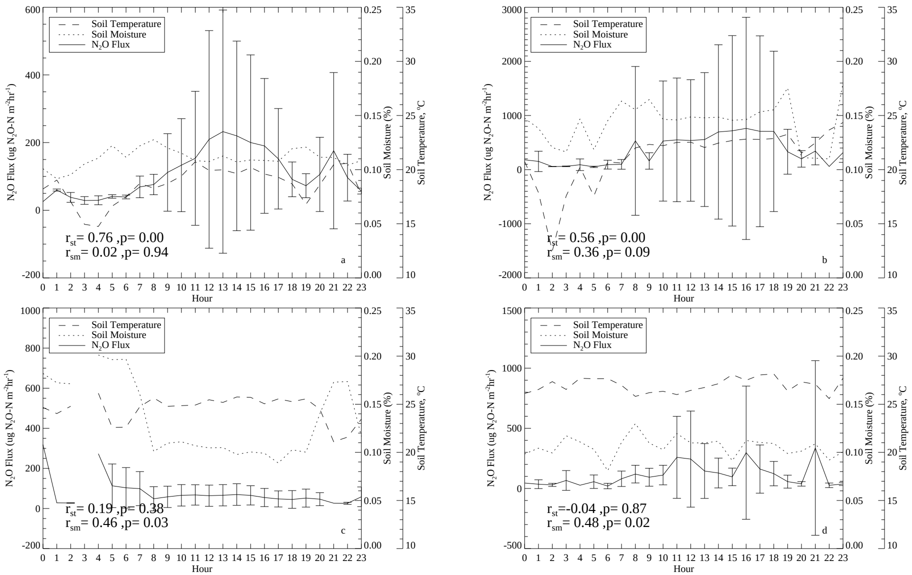

Figure 7. Diurnal variation of N_2O flux for the four sub-periods defined in Table 1, **(a)** the first period, **(b)** the second period, **(c)** the third period, and **(d)** the fourth period. r_{st} is the correlation coefficient of N_2O flux and soil temperature; r_{sm} is the correlation coefficient of N_2O flux and soil moisture.

ACPD
14, 20417–20460, 2014

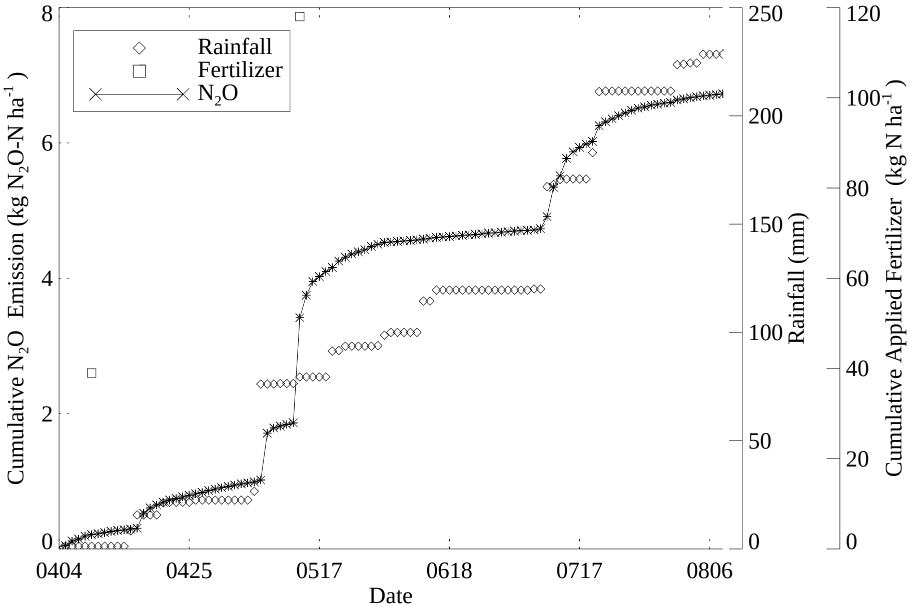

Figure 8. Cumulative N_2O emission for the experimental site, during 4 April to 8 August 2012. Rainfall and N fertilizer applications data were also shown, 24 days before the experiment (10 March) chicken litter was applied at a rate of 99 kg N ha^{-1}.

ACPD

14, 20417–20460, 2014

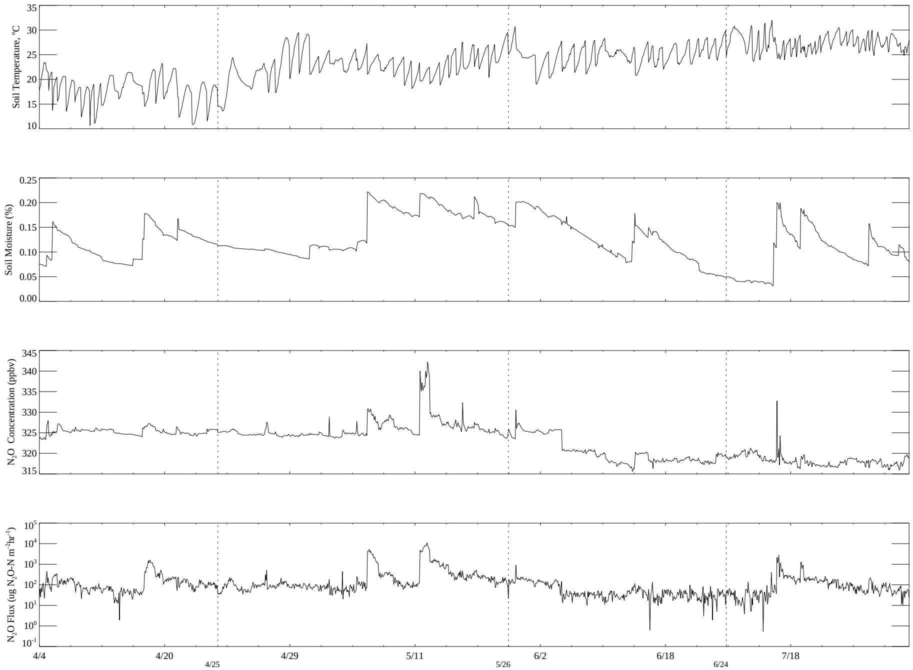

Figure 9. Time series of soil temperature, soil moisture, N_2O concentration, and flux for the whole experimental period. The vertical dashed lines indicate the sub-periods defined in Table 1.

ACPD
14, 20417–20460, 2014

Nitrous oxide emissions from a commercial cornfield

H. Huang et al.

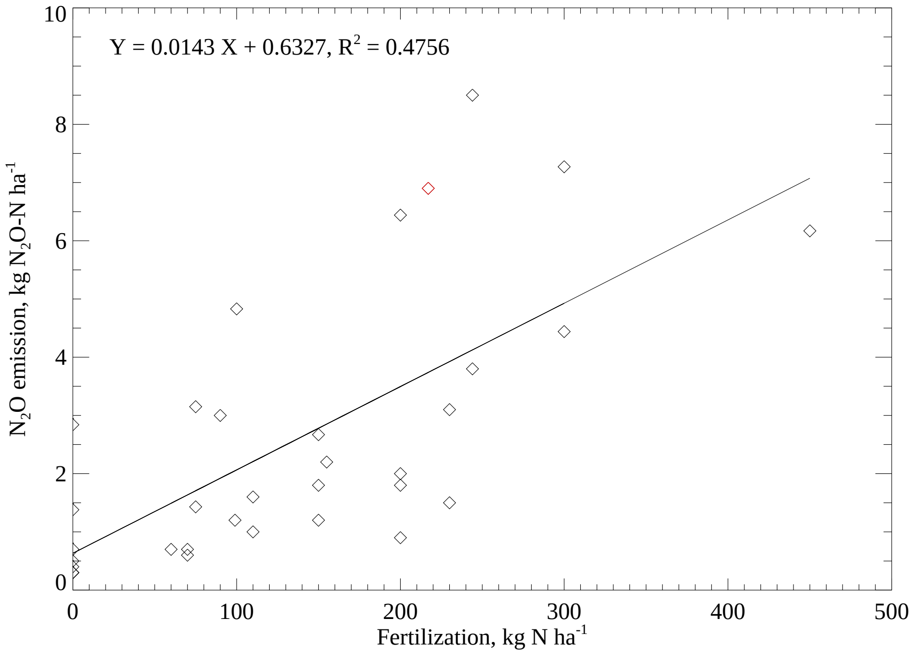

Figure 10. Regression of cumulative N_2O emission on the total applied fertilizer N in 10 different studies (where both amount of fertilizer and cumulative N_2O emission are provided) listed in Table 6, the result of this study is indicated by the red square.

ACPD
14, 20417–20460, 2014